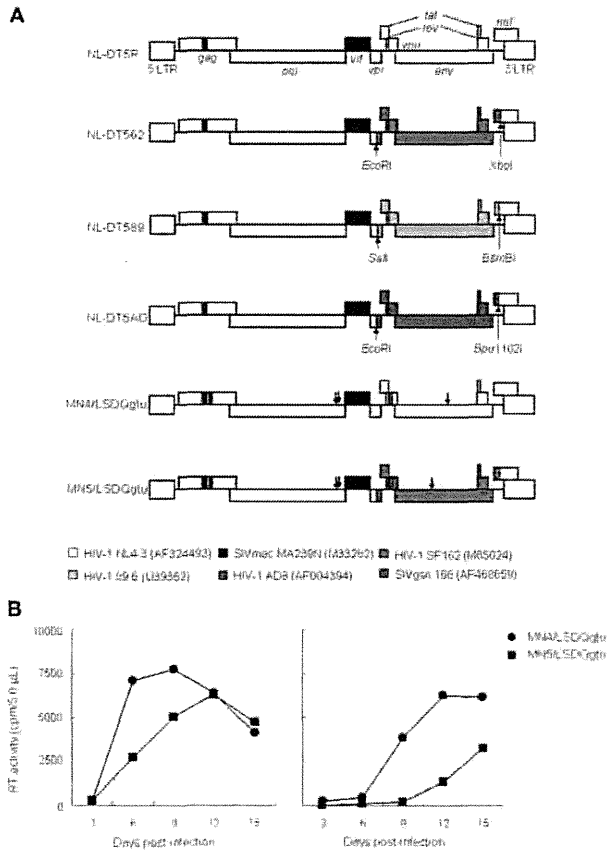

FIGURE 1 | Characteristics of HIV-1mt clones. (A) Proviral genome structure of various HIV-1mt clones. Genomes of various HIV-1mt clones generated in our laboratory are schematically illustrated. White and black (a small portion of *gag*-capsid and an entire *vif*) areas stand for the genomic regions of HIV-1 NL4-3 (Adachi et al., 1986) and SIVmac MA239N (Shibata et al., 1991; Doi et al., 2010), respectively. The other colored regions are the sequences derived from various SIV/HIV-1s as shown. Restriction enzyme sites used for the insertion of these sequences into NL-DT5R are also shown. GenBank accession numbers are indicated in parentheses. Arrows represent the adaptive mutation sites in *pol*-integrase and *env*-gp120 that enhance virus growth potentials (Nomaguchi et al., 2013b). While NL-DT5R and MN4/LSDQgtu are CXCR4-tropic viruses, NL-DT562, NL-DT5AD, and MN5/LSDQgtu are CCR5-tropic. Although examined in macaque cells, the growth ability of NL-DT589 is not yet proven (see text). mac, rhesus macaques; gsn, greater spot-nosed monkeys. **(B)** Viral replication kinetics in M1.3S cells. Cell-free viruses were prepared from 293T cells transfected with proviral clones indicated, and equal amounts [5×10^6 and 5×10^5 reverse transcriptase (RT) units for left and right panels, respectively] were inoculated into M1.3S cells (2×10^6 cells). Viral replication was monitored at intervals by RT activity in the culture supernatants. The experiments were done as described previously (Kamada et al., 2006). M1.3S is the most refractory cell line to infection with SIVmac/HIV-1mt clones to the best of our knowledge, but is CD4-, CXCR4-, and CCR5-positive. NL-DT5R and NL-DT562 do not grow at all in M1.3S cells.

of the replication ability of CCR5-tropic HIV-1mt clones would be necessary to establish HIV-1mt/macaque model systems, the rhesus system in particular, for natural infections of HIV-1, and finally for human AIDS research.

ACKNOWLEDGMENTS

We thank Ms. Kazuko Yoshida of our department for editorial assistance. We are indebted to Professor Tatsuhiko Igarashi of Kyoto University for his contribution to our study described here.

REFERENCES

Adachi, A., Gendelman, H. E., Koenig, S., Folks, T., Willey, R., Rabson, A., et al. (1986). Production of acquired immunodeficiency syndrome-associated retrovirus in human and nonhuman cells transfected with an infectious molecular clone. *J. Virol.* 59, 284–291.

Akari, H., Mori, K., Terao, K., Otani, I., Fukasawa, M., Mukai, R., et al. (1996). *In vitro* immortalization of Old World monkey T lymphocytes with *Herpesvirus saimiri*: its susceptibility to infection with simian immunodeficiency viruses. *Virology* 218, 382–388. doi: 10.1006/viro.1996.0207

Doi, N., Fujiwara, S., Adachi, A., and Nomaguchi, M. (2010). Growth ability in various macaque cell lines of HIV-1 with simian cell-tropism. *J. Med. Invest.* 57, 284–292. doi: 10.2152/jmi.57.284

Doi, N., Fujiwara, S., Adachi, A., and Nomaguchi, M. (2011). Rhesus M1.3S cells suitable for biological evaluation of macaque-tropic HIV/SIV clones. *Front. Microbiol.* 2:115. doi: 10.3389/fmicb.2011.00115

Feinberg, M. B., and Moore, J. P. (2002). AIDS vaccine models: challenging challenge viruses. *Nat. Med.* 3, 207–210. doi: 10.1038/nm0302-207

Fujita, M., Yoshida, A., Sakurai, A., Tatsuki, J., Ueno, F., Akari, H., et al. (2003). Susceptibility of HVS-immortalized lymphocytic HSC-F cells to various strains and mutants of HIV/SIV. *Int. J. Mol. Med.* 11, 641–644.

Fujita, Y., Otsuki, H., Watanabe, Y., Yasui, M., Kobayashi, T., Miura, T., et al. (2012). Generation of a replication-competent chimeric simian-human immunodeficiency virus carrying *env* from subtype C clinical isolate through intracellular homologous recombination. *Virology* 436, 100–111. doi: 10.1016/j.virol.2012.10.036

Hatziioannou, T., Ambrose, Z., Chung, N. P. Y., Piatak, M. Jr., Yuan, F., Trubey, C. M., et al. (2009). A macaque model of HIV-1 infection. *Proc. Natl. Acad. Sci. U.S.A.* 106, 4425–4429. doi: 10.1073/pnas.0812587106

Hatziioannou, T., Princiotta, M., Piatak, M. Jr., Yuan, F., Zhang, F., Lifson, J. D., et al. (2006). Generation of simian-tropic HIV-1 by restriction factor evasion. *Science* 314:95. doi: 10.1126/science.1130994

Hsu, M., Harouse, J. M., Gettie, A., Buckner, C., Blanchard, J., and Cheng-Mayer, C. (2003). Increased mucosal transmission but not enhanced pathogenicity of the CCR5-tropic, simian AIDS-inducing simian/human immunodeficiency virus SHIV (SF162P3) maps to envelope gp120. *J. Virol.* 77, 989–998. doi: 10.1128/JVI.77.2.989-998.2003

Humbert, M., Rasmussen, R. A., Song, R., Ong, H., Sharma, P., Chenine, A. L., et al. (2008). SHIV-1157i and passaged progeny viruses encoding R5 HIV-1 clade C *env* cause AIDS in rhesus monkeys. *Retrovirology* 5:94. doi: 10.1186/1742-4690-5-94

Igarashi, T., Iyengar, R., Byrum, R. A., Buckler-White, A., Dewar, R. L., Buckler, C. E., et al. (2007). Human immunodeficiency virus type 1 derivative with 7% simian immunodeficiency virus genetic content is able to establish infections in pig-tailed macaques. *J. Virol.* 81, 11549–11552. doi: 10.1128/JVI.00960-07

Kamada, K., Igarashi, T., Martin, M. A., Khamsri, B., Hatcho, K., Yamashita, T., et al. (2006). Generation of HIV-1 derivatives that productively infect macaque monkey lymphoid cells. *Proc. Natl. Acad. Sci. U.S.A.* 103, 16959–16964. doi: 10.1073/pnas.0608289103

Margolis, L., and Shattock, R. (2006). Selective transmission of CCR5-utilizing HIV-1: the 'gatekeeper' problem resolved? *Nat. Rev. Microbiol.* 4, 312–317.

Matsuda, K., Inaba, K., Fukazawa, Y., Matsuyama, M., Ibuki, K., Horiike, M., et al. (2010). *In vivo* analysis of a new R5 tropic SHIV generated from the highly pathogenic SHIV-KS661, a

derivative of SHIV-89.6. *Virology* 399, 134–143. doi: 10.1016/j.virol.2010.01.008

Nishimura, Y., Shingai, M., Willey, R., Sadjadpour, R., Lee, W. R., Brown, C. R., et al. (2010). Generation of the pathogenic R5-tropic simian/human immunodeficiency virus $SHIV_{AD8}$ by serial passaging in rhesus macaques. *J. Virol.* 84, 4769–4781. doi: 10.1128/JVI.02279-09

Nomaguchi, M., Doi, N., Fujiwara, S., and Adachi, A. (2011). "Macaque-tropic HIV-1 derivatives: a novel experimental approach to understand viral replication and evolution *in vivo*," in *HIV-Host Interactions*, ed T. L.-Y. Chang (Rijeka: InTech), 325–348.

Nomaguchi, M., Doi, N., Kamada, K., and Adachi, A. (2008). Species barrier of HIV-1 and its jumping by virus engineering. *Rev. Med. Virol.* 18, 261–275. doi: 10.1002/rmv.576

Nomaguchi, M., Yokoyama, M., Kono, K., Nakayama, E. E., Shioda, T., Saito, A., et al. (2013a). Gag-CA Q110D mutation elicits TRIM5-independent enhancement of HIV-1mt replication in macaque cells. *Microbes Infect.* 15, 56–65.

Nomaguchi, M., Doi, N., Fujiwara, S., Saito, A., Akari, H., Nakayama, E. E., et al. (2013b). Systemic biological analysis of the mutations in two distinct HIV-1mt genomes occurred during replication in macaque cells. *Microbes Infect.* 15, 319–328.

Saito, A., Nomaguchi, M., Iijima, S., Kuroishi, A., Yoshida, T., Lee, Y. J., et al. (2011). Improved capacity of a monkey-tropic HIV-1 derivative to replicatein cynomolgus monkeys with minimal modifications. *Microbes Infect.* 13, 58–64. doi: 10.1016/j.micinf.2010.10.001

Saito, A., Nomaguchi, M., Kono, K., Iwatani, Y., Yokoyama, M., Yasutomi, Y., et al. (2013). *TRIM5* genotypes in cynomolgus monkeys primarily influence inter-individual diversity in susceptibility to monkey-tropic human immunodeficiency virus type 1. *J. Gen. Virol.* 94, 1318–1324. doi: 10.1099/vir.0.050252-0

Shibata, R., Kawamura, M., Sakai, H., Hayami, M., Ishimoto, A., and Adachi, A. (1991). Generation of a chimeric human and simian immunodeficiency virus infectious to monkey peripheral blood mononuclear cells. *J. Virol.* 65, 3514–3520.

Thippeshappa, R., Polacino, P., Kimata, M. T. Y., Siwak, E. B., Anderson, D., Wang, W., et al. (2011). Vif substitution enables persistent infection of pig-tailed macaques by human immunodeficiency virus type 1. *J. Virol.* 85, 3767–3779. doi: 10.1128/JVI.02438-10

Received: 09 July 2013; accepted: 12 July 2013; published online: 29 July 2013.

Citation: Doi N, Okubo A, Yamane M, Sakai Y, Adachi A and Nomaguchi M (2013) Growth potentials of CCR5-tropic/CXCR4-tropic HIV-1mt clones in macaque cells. Front. Microbiol. 4:218. doi: 10.3389/fmicb.2013.00218

This article was submitted to Frontiers in Virology, a specialty of Frontiers in Microbiology.

Virology 449 (2014) 82–87

Contents lists available at ScienceDirect

Virology

journal homepage: www.elsevier.com/locate/yviro

Defining HIV-1 Vif residues that interact with CBFβ by site-directed mutagenesis

Yusuke Matsui [a], Keisuke Shindo [a,*], Kayoko Nagata [a], Katsuhiro Io [a], Kohei Tada [a], Fumie Iwai [a], Masayuki Kobayashi [a], Norimitsu Kadowaki [a], Reuben S. Harris [b,c], Akifumi Takaori-Kondo [a]

[a] Department of Hematology and Oncology, Graduate School of Medicine, Kyoto University, Kyoto 606-8507, Japan
[b] Department of Biochemistry, Molecular Biology and Biophysics, University of Minnesota, MN 55455, United States
[c] Institute for Molecular Virology, University of Minnesota, MN 55455, United States

ARTICLE INFO

Article history:
Received 28 August 2013
Returned to author for revisions
13 September 2013
Accepted 1 November 2013
Available online 26 November 2013

Keywords:
HIV-1
Vif
CBFβ
Interaction
Host factors

ABSTRACT

Vif is essential for HIV-1 replication in T cells and macrophages. Vif recruits a host ubiquitin ligase complex to promote proteasomal degradation of the APOBEC3 restriction factors by poly-ubiquitination. The cellular transcription cofactor CBFβ is required for Vif function by stabilizing the Vif protein and promoting recruitment of a cellular Cullin5-RING ubiquitin ligase complex. Interaction between Vif and CBFβ is a promising therapeutic target, but little is known about the interfacial residues. We now demonstrate that Vif conserved residues E88/W89 are crucial for CBFβ binding. Substitution of E88/W89 to alanines impaired binding to CBFβ, degradation of APOBEC3, and virus infectivity in the presence of APOBEC3 in single-cycle infection. In spreading infection, NL4-3 with Vif E88A/W89A mutation replicated comparably to wild-type virus in permissive CEM-SS cells, but not in multiple APOBEC3 expressing non-permissive CEM cells. These results support a model in which HIV-1 Vif residues E88/W89 may participate in binding CBFβ.

Introduction

HIV-1 Vif is one of six viral accessory proteins and it is essential for the viral replication in T cells and macrophages (Gabuzda et al., 1992, 1994). Vif recruits host proteins, cullin 5 (CUL5), RING-box protein 2 (RBX2), elongin C (ELOC) and elongin B (ELOB), and forms a ubiquitin ligase complex that promotes poly-ubiquitination and proteasomal degradation of the APOBEC3 (A3) retrovirus restriction factors (Jäger et al., 2011; Marin et al., 2003; Sheehy et al., 2003; Shirakawa et al., 2006; Stopak et al., 2003; Yu et al., 2003). A3s are DNA cytosine deaminases that convert cytosines to uracils in single-stranded DNA (Chelico et al., 2006; Harris et al., 2003). In the absence of the Vif protein, at least two A3 family members, A3F and A3G, are efficiently incorporated into budding virions, where they deaminate cytosines in newly reverse-transcribed minus-strand virus DNA in target cells, leading to guanine to adenine hypermutation of the virus genome (Harris et al., 2003; Hultquist et al., 2011b; Sheehy et al., 2002; Zhang et al., 2003).

Amino acid sequences of HIV-1 Vif vary among viral strains, but more than ten regions of residues are conserved (Dang et al., 2010), and several conserved motifs have been shown to interact with host proteins. The BC-box motif ^{144}SLQYLA^{149} binds to ELOC (Mehle et al., 2004; Yu et al., 2004), and the HCCH motif ^{108}Hx$_5$Cx$_{17-18}$Cx$_{3-5}$H^{139} binds to CUL5 (Luo et al., 2005; Mehle et al., 2006). Furthermore, the N-terminal half of Vif contains distinct regions involved in the Vif-A3 protein-protein interactions; ^{11}WQxDRMR^{17} and ^{76}ExxW^{79} motifs are involved in neutralization of A3F (He et al., 2008; Russell and Pathak, 2007), whereas ^{40}YRHHY^{44} motif is involved in neutralization of A3G (Russell and Pathak, 2007); ^{22}KSLVK^{26} and ^{55}VxIPLx4-5Lxφx2YWxL^{72} motifs were reported to be involved in neutralization of both A3F and A3G (Chen et al., 2009; Dang et al., 2009; He et al., 2008; Pery et al., 2009), although there exists a report that K26 is required for neutralization of A3G, but not of A3F (Albin et al., 2010).

Recently, the transcription factor core binding factor-β (CBFβ) has been shown to be involved in the Vif ubiquitin ligase complex (Jäger et al., 2011; Zhang et al., 2011), and critical for its function by stabilizing the Vif protein in cells (Jäger et al., 2011), and enabling the recruitment of CUL5 (Zhang et al., 2011). There are two isoforms of CBFβ, and both isoforms stabilize Vif protein, enhance A3 degradation, and increase virion infectivity (Hultquist et al., 2011a). Thus, the interaction between Vif and CBFβ is a promising

* Correspondence to: Department of Hematology and Oncology, Graduate School of Medicine, 54 Shogoin-Kawaracho, Sakyo-ku, Kyoto, 606-8507 Japan.
Tel: +81 75 751 4964. Fax: +81 75 751 4963.
E-mail address: shind009@kuhp.kyoto-u.ac.jp (K. Shindo).

0042-6822/$ - see front matter © 2013 Elsevier Inc. All rights reserved.
http://dx.doi.org/10.1016/j.virol.2013.11.004

therapeutic target, but little is known about the interfacial amino acids. Hultquist et al. reported that surface F68 residue of CBFβ is involved in binding and stabilizing Vif (Hultquist et al., 2012). Zhang et al. reported that W21 and W38 residues of Vif are required for binding to CBFβ by co-immunoprecipitation experiments (Zhang et al., 2011; Kim et al., 2013). Furthermore, Kim et al. recently suggested that L64 and I66 residues are involved in binding to CBFβ by co-purification in *Escherichia coli* (Kim et al., 2013).

Because a previous study indicated that a hydrophilic region ^{88}EWRKKR^{93} is essential for Vif expression and HIV-1 replication (Fujita et al., 2003), we hypothesized that conserved residues E88 and W89 in this region may be required for CBFβ binding. In this study, we generated amino acid substitution mutants of these residues as well as W21 and W38, and simultaneously analyzed both binding to CBFβ and Vif-mediated degradation of A3F and A3G. We show that the conserved residues E88 and W89 of HIV-1 Vif are directly involved in CBFβ binding and Vif-mediated degradation of A3F and A3G.

Results

The conserved residue W89 of HIV-1 Vif is required for the interaction with CBFβ

To test our hypothesis that conserved residues E88 and W89 may be required for CBFβ binding, we generated nine Vif amino acid substitution mutants, D14A/R15A, W21A, W38A, Y40A, Y69A, G84D, E88A, W89A, and E88A/W89A (Fig. 1A). W21 and W38 were reported to be involved in CBFβ binding (Zhang et al., 2011), D14 and R15 for APOBEC3F binding (Russell and Pathak, 2007), Y40 for A3G binding (Russell and Pathak, 2007), Y69 and G84 for both A3F and A3G binding (Dang et al., 2010; Pery et al., 2009). All of these residues are highly conserved, suggesting that they could be involved in CBFβ binding region of Vif. We first performed co-immunoprecipitation experiments in 293T cells by over-expression of Vif with C-terminal myc tag. Vif is a relatively unstable protein with a short half-life and it is degraded by the cellular proteasome (Dussart et al., 2004; Fujita et al., 2004; Mehle et al., 2004). Mouse double minute 2 homolog (MDM2) is the E3 ubiquitin ligase which targets Vif for degradation (Izumi et al., 2009). Because it has been reported that Vif degradation is accelerated in the absence of CBFβ, and that treatment with the proteasome inhibitor MG132 reverses this effect (Jäger et al., 2011), we used MG132 to minimize proteasomal proteolysis of Vif in cell culture and immunoprecipitation experiments. Although we transfected with the same amount of plasmid DNA, expression levels of E88A, W38A, D14/R15AA, Y40A, Y69A and G84D were comparable to wild-type Vif, but those of W89A, E88/W89A and W21A mutants were obviously impaired (Fig. S1, 2nd top panel). These modest expression levels of these mutants can be simply explained by misfolding, but an alternative explanation is due to loss of CBFβ binding. The amounts of immunoprecipitated Vif protein showed a smaller variation, compared to expression levels (Fig. S1, bottom panel). More importantly, endogenous CBFβ co-precipitated with wild-type Vif, D14A/R15A, Y40A, G84D, and E88A, but not with W21A, W89A, or E88A/W89A (Fig. S1, 3rd top panel). W38A and Y69A showed intermediate results (Fig. S1, lanes 7 and 10, 3rd top panel). To exclude the possibility that low expression of W21A, W89A and E88A/W89A mutants caused the low amount of co-immunoprecipitated CBFβ, we compensated by increasing the amount of transfected plasmid DNA, and performed an additional round of co-immunoprecipitation experiments. Although expression levels of W21A, W89A and E88A/W89A mutants were now higher than wild-type Vif, endogenous CBFβ did not co-precipitate with these mutants (Fig. 1B). We next examined whether CUL5 co-precipitated with Vif mutants by immunoblotting with some of the samples of Fig. 1B, because CBFβ binding has been reported to be required for Vif to interact with CUL5 (Zhang et al., 2011). Endogenous CUL5 appeared to co-precipitate with wild-type Vif, but not with W21A, W38A, W89A, or E88A/W89A (Fig. 1C, 2nd bottom panel). All

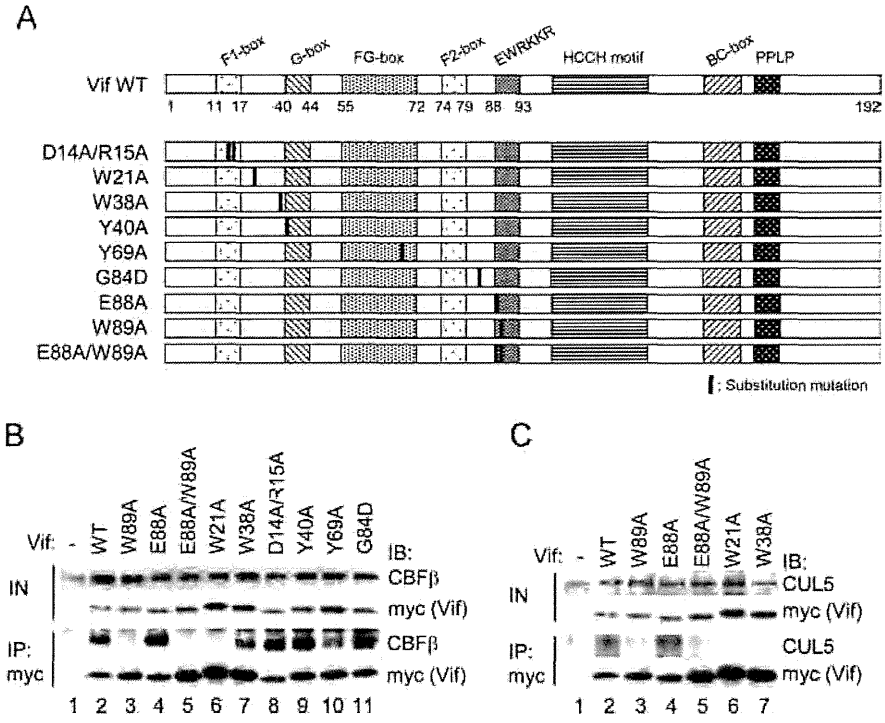

Fig. 1. Vif substitution mutants and binding capacity to CBFβ. (A) Schematic of Vif conserved motifs and nine substitution mutants generated. The residues substituted are indicated by bold lines. (B) Co-immunoprecipitation of endogenous CBFβ with Vif. Lysates of 293T cells transiently expressing myc-tagged Vif wild-type or mutant were immunoprecipitated by anti-myc serum. Samples were analyzed by immunoblotting with anti-CBFβ and anti-myc sera. (C) Co-immunoprecipitation of endogenous CUL5 with Vif. Samples from (B) were also analyzed with anti-CUL5 serum. Panels for Vif were re-produced from (B).

of these mutants of Vif bound to ELOB (Fig. S2), suggesting that they are not entirely misfolded proteins, although previous reports indicated that fragments of the Vif BC box is sufficient for binding to ELOB and ELOC (Bergeron et al., 2010; Wolfe et al., 2010). Altogether, these results suggest that W89 is involved in CBFβ binding, as well as W21 and W38.

The substitution of E88/W89 to alanines impairs Vif-mediated degradation of both A3F and A3G proteins

To examine whether the loss of binding to CBFβ causes impaired Vif-mediated degradation of A3 proteins, we next performed a series of co-transfection and immunoblot experiments. 293T cells were co-transfected with expression vectors for A3G with myc tag and Vif wild-type or mutant, and protein levels of A3G were analyzed by immunoblotting. To obtain comparable expression levels of each of the Vif mutants, we again adjusted the amount of plasmid DNA transfected. Co-transfection of wild-type Vif reduced APOBEC3G levels, but E88A/W89A, W21A or W38A did not (Fig. 2A, lanes 1, 2 and 7–12). E88A or W89A alone reduced A3G levels close to wild-type Vif (Fig. 2A, lanes 3–6). Because W21 and W38 are close to A3G binding residues of Vif, ^{40}YRHHY^{44}, the loss of A3G degradation by W21A or W38A might be caused by loss of A3G binding. To exclude this possibility, we next performed co-transfection experiments with Vif and A3F expression vectors and similar results were obtained (Fig. 2B). These results suggest that the substitution of E88/W89 as well as W21 and W38 to alanines leads to an impairment of Vif-mediated degradation of both A3F and A3G due to the loss of binding to CBFβ, not to A3F or A3G.

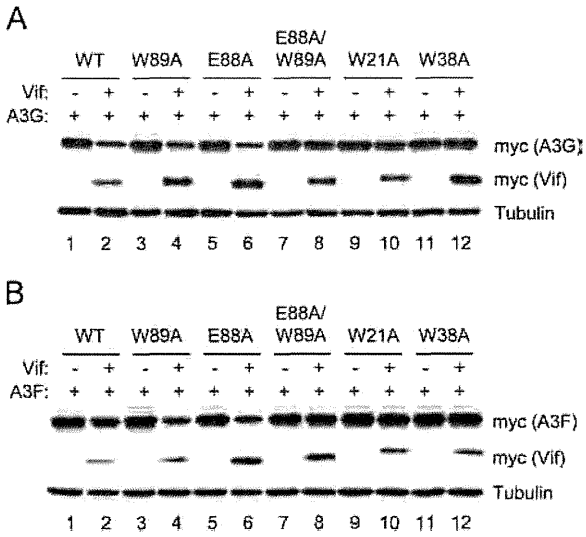

Fig. 2. Degradation of A3F and A3G by Vif. (A) Degradation of A3G. HEK293T cells were co-transfected with expression vectors for myc-tagged A3G and Vif wild-type or mutant, and protein levels of A3G and Vif were analyzed by immunoblotting with anti-myc serum and anti-tubulin antibody for loading control. The same amount of the A3G expression plasmid was transfected in each sample. (B) Degradation of A3F. Similar experiments to (A), but an A3F expression vector was used instead of that of A3G.

The substitution of E88/W89 to alanines impairs the ability of Vif to counteract the restriction by both A3F and A3G

To examine the ability of Vif mutants to counteract the restriction of HIV-1 by A3 proteins, we next performed single cycle infection experiments using luciferase-reporter viruses. The Vif mutations were introduced into pNL4-3 ΔEnv-Luc, and transfected into 293T cells with co-transfection of VSV-G expression plasmid in the presence or absence of co-transfection of A3G expression plasmid. Virus-containing supernatant was harvested and infectivity was measured by challenging to fresh 293T cells and assaying luciferase activity. Viruses with Vif mutations showed comparable infectivity in the absence of A3G, as expected (Fig. 3A). In the presence of A3G, virus with E88A mutation showed comparable infectivity to wild-type, but virus with W21A, W38A or E88A/W89A showed deeply impaired infectivity close to that of ΔVif (Fig. 3A). Virus with W89A showed intermediate and obviously impaired infectivity in the presence of A3G (Fig. 3A). We also performed these assays with A3F instead of A3G, and obtained similar results (Fig. 3B). These data indicate that E88/W89 residues as well as W21 and W38 are involved in Vif activity to counteract both A3F and A3G, suggesting these residues are involved in CBFβ binding, not A3F or A3G binding.

The substitution of E88/W89 to alanines impairs HIV-1 replication in non-permissive CEM cells

Finally, we performed spreading infection experiments in both permissive CEM-SS and multiple A3-expressing CEM cells. We introduced Vif mutations into NL4-3, a replication-competent

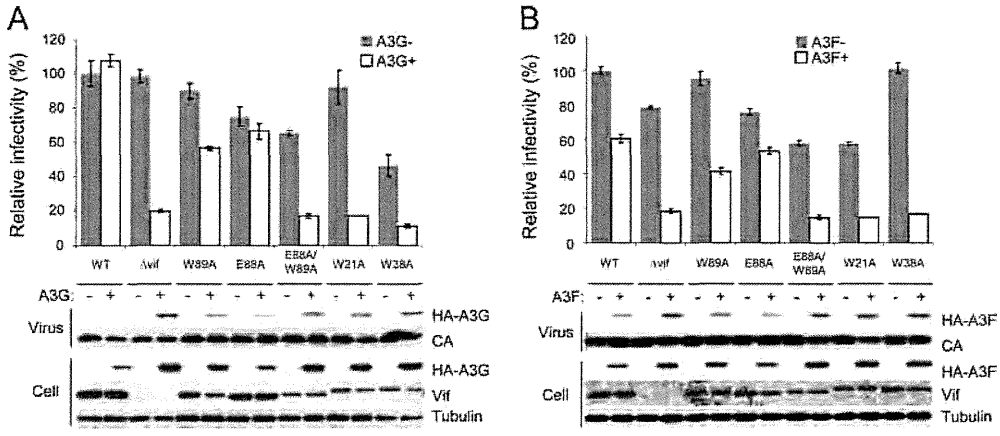

Fig. 3. Single-cycle infection experiments with VSV-G pseudo-typed viruses with vif mutations. (A) Counteracting abilities of Vif mutants against the restriction by A3G. 293T cells were transfected with pNL43/ΔEnv-Luc with vif mutation, together with pVSV-G, in the presence or absence of pcDNA3/HA-A3G. pNL43/ΔEnv-Luc without vif mutation and pNL43/ΔEnvΔvif-Luc were also used for control. Virus-containing supernatant was challenged to fresh 293T cells and infectivity was determined by luminometer. Values were normalized to that of the virus without vif mutation in the absence of A3G. Average and standard errors of 3 independent experiments are shown. Levels of A3G in cells and virions and Vif in cells were also analyzed by immunoblotting. (B) Counteracting abilities of Vif mutants against the restriction by A3F. Similar experiments to (A), but pcDNA3/HA-A3F was used instead of the A3G plasmid.

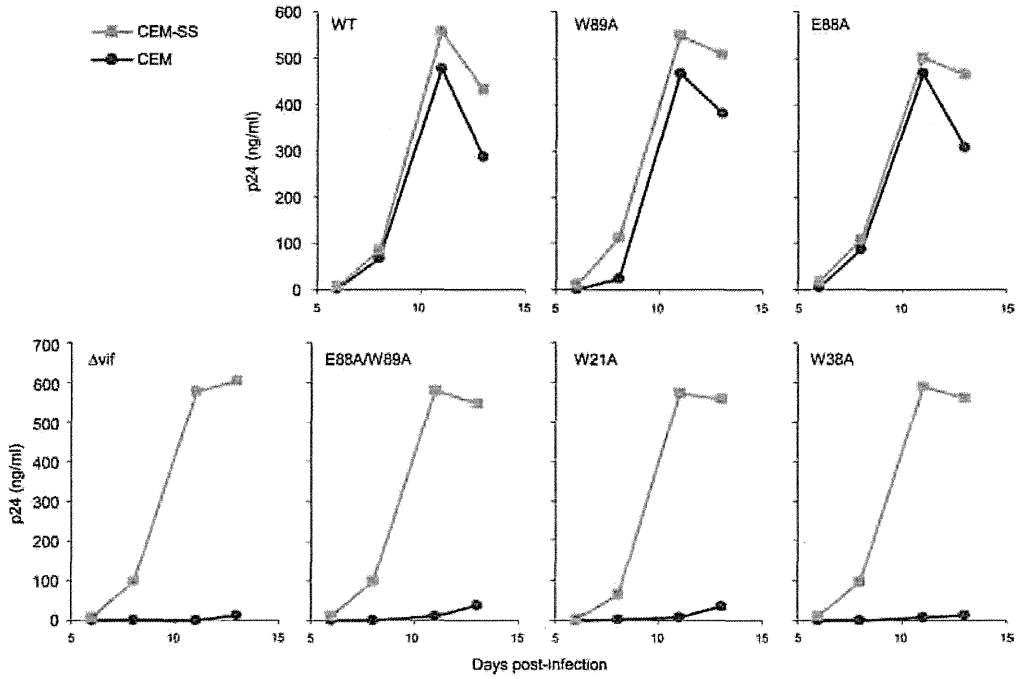

Fig. 4. *Spreading infection of NL4-3 with vif mutations. The viruses were produced in 293T cells and challenged to permissive CEM-SS cells and nonpermissive CEM cells at MOI of 0.005. Culture supernatant was collected periodically and p24 levels were determined by ELISA.*

molecular clone, and analyzed whether the substitution mutation impairs virus replication with spreading infection assays. Virus with E88A or W89A showed comparable replication profiles to wild-type virus in both CEM-SS and CEM cells. Virus with ΔVif, E88A/W89A, W21A, or W38A showed indistinguishable replication profiles to wild type in CEM-SS cells, as expected, whereas in CEM cells, showed deeply impaired replication profiles (Fig. 4). These results indicate that the residues E88/W89 as well as W21 and W38 are critical for Vif to counteract multiple A3s, suggesting that these residues are directly involved in CBFβ binding.

Discussion

In this study, we report that HIV-1 Vif residues E88 and W89 are involved in CBFβ binding, therefore in rendering Vif capable of stable expression and inducing ubiquitination of both A3F and A3G proteins. Fujita et al. reported that deletion or substitution of these residues impairs steady-state levels of Vif protein and virus replication in nonpermissive H9 cells and monocyte-derived macrophages (Fujita et al., 2003). We confirmed lower expression levels of substitution mutants using both Vif expression vectors and molecular clones of HIV-1. We also confirmed inefficient replication of virus with the mutation using another nonpermissive T cell line, CEM cells. These observations may be all explained by the loss of CBFβ binding.

Our results suggest that the single amino acid substitution mutant W89A does not bind to CBFβ, however this mutant is capable of degradation of A3F and A3G, and supporting replication of the virus in non-permissive CEM cells. This modest conflict may be due to the differences in experimental settings; co-immunoprecipitation experiments test the interactions *in vitro* in complex total cell lysates, and degradation experiments and infectivity experiments test Vif functionality in living cells.

Zhang et al. reported that Vif residues W21 and W38 are involved in binding to CBFβ, but functional correlation of these residues was not described (Zhang et al., 2011). We confirmed that these residues are critical for CBFβ binding, and further demonstrated that these residues are critical for degradation of both A3F and A3G, counteracting restriction by both A3F and A3G, and replication in nonpermissive, multiple A3-expressing cells.

Jäger et al. reported that CBFβ functions to up-regulate steady-state level of Vif protein by using cells with CBFβ knock-down (Jäger et al., 2011). We observed that the levels of Vif mutants that do not bind to CBFβ were obviously lower than that of wild-type Vif. Our observations confirmed and support the Jäger's report by the experiments with different settings.

Several E3 ligases including CUL5, NEDD4, and AIP4, have been reported to induce Vif ubiquitination, although biological implications have not been well defined (Dussart et al., 2004; Mehle et al., 2004). We previously reported that MDM2 targets for Vif as an E3 ligase to induce its ubiquitination and proteasomal degradation, and that the N-terminal region of Vif (residues 4–22) is required for MDM2 binding (Izumi et al., 2009). Because one of the CBFβ binding residues of Vif, W21, is located close to MDM2 binding region, the loss of CBFβ binding might facilitate ubiquitination and degradation of Vif by MDM2. Further investigations will be required to test this possibility.

We provide here the evidence indicating that residues W21, W38, E88 and W89 of HIV-1 Vif are involved in binding surface to CBFβ. Further studies on the Vif-CBFβ co-crystal structure will be the key to understanding Vif-CBFβ interaction surfaces, and to pharmaceutical applications of these pieces of information for patients with HIV-1 infection.

Materials and methods

Plasmid construction

C-terminally myc-tagged Vif expression plasmid, pDON-Vif-myc, was generated by amplifying NL4-3 vif coding sequence with primers ATA GGA TCC ATG GAA AAC AGA TG G CAG GTG GCA GGT GAT G and CGC GTC GAC CTA CAG ATC CTC TTC AGA GAT GAG TTT CTG CTC GTA GTG TCC ATT CAT TGT ATG GCT CCC, and inserting it into pDON-AI (Takara) at BamH I/Sal I sites. Expression plasmids for

Vif mutants were generated by a PCR-based method with properly mutated primers. HA-tagged expression plasmids for A3F and A3G were previously described (Shirakawa et al., 2006). N-terminally myc-tagged expression plasmids for A3F, pcDNA3-myc-A3F, was generated by amplifying coding sequences of human A3F with primers CTA GCT AGC ATG GAG CAG AAA CTC ATC TCT GAA GAG GAT CTG ATG AAG CCT CAC TTC AGA AAC ACA GTG G and GGG GTA CCT CAC TCG AGA ATC TCC TGC AGC TTG CTG, and inserting it into pcDNA3.1 (Invitrogen) at Nhe I/Kpn I sites. C-terminally myc-tagged expression plasmids for A3G, pcDNA3-A3G-myc, was generated by amplifying coding sequences of human A3G with primers ATA CTC GAG AAT GAA GCC TAC TTC AGA AAC ACA GTG and GGG GTA CCC TAC AGA TCC TCT TCA GAG ATG AGT TTC TGC TCG CAG TTT TCC TGA TTC TGG AGA ATG GC, and inserting it into pcDNA3.1 (Invitrogen) at Xho I/Kpn I sites. The luciferase-reporter HIV-1 plasmids for single-cycle infection, pNL43/ΔEnv-Luc and pNL43/ΔEnvΔvif-Luc were previously described (Shindo et al., 2003). Mutations in vif region of pNL43/ΔEnv-Luc and pNL4-3 were introduced by a PCR-based method using internal restriction sites, MSC I at position 4553, and EcoR I at position 5743.

Cell culture and transfection

293T cells were maintained in Dulbecco's modified Eagle's medium supplemented with 10% fetal bovine serum (FBS) and penicillin, streptomycin and glutamine (PSG). CEM and CEM-SS cells were maintained in RPMI1640 medium supplemented with 10% FBS and PSG. 293T cells on 6-well plates were transfected with about 1 μg of plasmid DNA in total using X-tremegene HP DNA transfection reagent (Roche) according to manufacturer's instruction.

Immunoblotting

Primary antibodies for immunoblotting against Vif, A3G and $p24^{Gag}$ were obtained from the NIH AIDS Research and Reference Reagent Program. Rabbit anti-CBFβ serum and mouse anti-Cul5 and anti-HA antibodies were purchased from Santa Cruz. Rabbit anti-myc serum was purchased from Sigma. Mouse anti-tubulin antibody was purchased from Covance. HRP-conjugated secondary antibodies against mouse and rabbit were purchased from GE Healthcare. We used a standard chemiluminescence protocol for immunoblotting with PVDF membrane (Millipore).

Immunoprecipitation

For co-immunoprecipitation to test interaction of Vif mutant to CBFβ, 293T cells were transfected with pDON-Vif-myc or its derivative mutant, treated with MG132 at concentration of 2.5 μM for 16 h, and lysed with co-IP buffer (25 mM HEPES, pH 7.4, 150 mM NaCl, 0.1% Triton X-100, 1 mM EDTA, 1mM $MgCl_2$) supplemented with protease inhibitor cocktail (Nacalai) and MG132. After centrifugation at 20,000 × *g* for 10 min, supernatant was mixed with 2 μg anti-myc rabbit serum (Sigma) for 1 h, and then mixed with 20 μl protein A sepharose (Pharmacia) for 1 h. Beads were washed with co-IP buffer 3 times, and bound protein was eluted with 1 x SDS sample buffer. Samples were analyzed by immunoblotting as described above.

Single-cycle infection

Luciferase encoding HIV-1 particles were produced by transiently transfecting 293T cells at 50% confluency using 0.8 μg pNL43/ΔEnv-Luc or derivative mutant, 0.2 μg pVSV-G and 0.02 μg pcDNA3/HA-A3F, pcDNA3/HA-A3G, or empty vector. After 48 h, virus-containing supernatants were harvested through PVDF filter with 0.45 μm pores (Millipore), and challenged to fresh 293T cells. After 48 h, cells were lysed with Passive lysis buffer (Promega) and luciferase activity was determined by luminometer (2030 Arvo X, Perkin Elmer) using Luciferase Assay System (Promega). Sample preparation of producer cells and virus for immunoblotting was performed as described (Haché et al., 2008).

Spreading infection

293T cells were transfected with NL4-3 molecular clone or derivative mutant, and virus-containing supernatant was harvested through PVDF filters with 0.45 μm pores (Millipore) after 2-day incubation. CEM-SS and CEM cells were inoculated with the supernatant at MOI of 0.005. The culture supernatants were harvested periodically, and analyzed for p24 by an HIV-1 p24 antigen ELISA kit (Zeptometrix).

Acknowledgments

We thank Dr. Y. Koyanagi for BL3 laboratory, Drs. J. Hultquist and A. Land in University of Minnesota for helpful discussion. The following materials were obtained through the AIDS Research and Reference Reagent Program, NIH: rabbit anti-Vif serum 2221 from Dr. Dana Gabuzda, anti-p24 Gag monoclonal antibody 6457 from Dr. Michael H. Malim, and rabbit anti-A3G serum 10201 from Dr. Jaisri Lingappa.

This study was partly supported by Grants-in-aid from the Ministry of Education, Culture, Sports, Science and Technology and from the Ministry of Health, Labor and Welfare in Japan. Work in the Harris lab was supported in part by grants from the National Institutes of Health (R01 AI064046 and P01 GM091743).

Appendix A. Supplementary material

Supplementary data associated with this article can be found in the online version at http://dx.doi.org/10.1016/j.virol.2013.11.004.

References

Albin, J.S., Haché, G., Hultquist, J.F., Brown, W.L., Harris, R.S., 2010. Long-term restriction by APOBEC3F selects human immunodeficiency virus type 1 variants with restored Vif function. J. Virol. 84 (19), 10209–10219.

Bergeron, J.R., Huthoff, H., Veselkov, D.A., Beavil, R.L., Simpson, P.J., Matthews, S.J., Malim, M.H., Sanderson, M.R., 2010. The SOCS-box of HIV-1 Vif interacts with ElonginBC by induced-folding to recruit its Cul5-containing ubiquitin ligase complex. PLoS Pathog 6 (6), e1000925.

Chelico, L., Pham, P., Calabrese, P., Goodman, M.F., 2006. APOBEC3G DNA deaminase acts processively 3′→5′ on single-stranded DNA. Nat. Struct. Mol. Biol. 13 (5), 392–399.

Chen, G., He, Z., Wang, T., Xu, R., Yu, X.F., 2009. A patch of positively charged amino acids surrounding the human immunodeficiency virus type 1 Vif SLVx4Yx9Y motif influences its interaction with APOBEC3G. J. Virol. 83 (17), 8674–8682.

Dang, Y., Davis, R.W., York, I.A., Zheng, Y.H., 2010. Identification of 81LGxGxxIxW89 and 171EDRW174 domains from human immunodeficiency virus type 1 Vif that regulate APOBEC3G and APOBEC3F neutralizing activity. J. Virol. 84 (11), 5741–5750.

Dang, Y., Wang, X., Zhou, T., York, I.A., Zheng, Y.H., 2009. Identification of a novel WxSLVK motif in the N terminus of human immunodeficiency virus and simian immunodeficiency virus Vif that is critical for APOBEC3G and APOBEC3F neutralization. J. Virol. 83 (17), 8544–8552.

Dussart, S., Courcoul, M., Bessou, G., Douaisi, M., Duverger, Y., Vigne, R., Decroly, E., 2004. The Vif protein of human immunodeficiency virus type 1 is posttranslationally modified by ubiquitin. Biochem. Biophys. Res. Commun. 315 (1), 66–72.

Fujita, M., Akari, H., Sakurai, A., Yoshida, A., Chiba, T., Tanaka, K., Strebel, K., Adachi, A., 2004. Expression of HIV-1 accessory protein Vif is controlled uniquely to be low and optimal by proteasome degradation. Microb. Infect. 6 (9), 791–798.

Fujita, M., Sakurai, A., Yoshida, A., Miyaura, M., Koyama, A.H., Sakai, K., Adachi, A., 2003. Amino acid residues 88 and 89 in the central hydrophilic region of human immunodeficiency virus type 1 Vif are critical for viral infectivity by enhancing the steady-state expression of Vif. J. Virol. 77 (2), 1626–1632.

Gabuzda, D.H., Lawrence, K., Langhoff, E., Terwilliger, E., Dorfman, T., Haseltine, W.A., Sodroski, J., 1992. Role of vif in replication of human immunodeficiency virus type 1 in CD4+ T lymphocytes. J. Virol. 66 (11), 6489–6495.

Gabuzda, D.H., Li, H., Lawrence, K., Vasir, B.S., Crawford, K., Langhoff, E., 1994. Essential role of vif in establishing productive HIV-1 infection in peripheral

blood T lymphocytes and monocyte/macrophages. J. Acquir. Immune Defic. Syndr. 7 (9), 908–915.
Haché, G., Shindo, K., Albin, J.S., Harris, R.S., 2008. Evolution of HIV-1 isolates that use a novel Vif-independent mechanism to resist restriction by human APOBEC3G. Curr. Biol. 18 (11), 819–824.
Harris, R.S., Bishop, K.N., Sheehy, A.M., Craig, H.M., Petersen-Mahrt, S.K., Watt, I.N., Neuberger, M.S., Malim, M.H., 2003. DNA deamination mediates innate immunity to retroviral infection. Cell 113 (6), 803–809.
He, Z., Zhang, W., Chen, G., Xu, R., Yu, X.F., 2008. Characterization of conserved motifs in HIV-1 Vif required for APOBEC3G and APOBEC3F interaction. J. Mol. Biol. 381 (4), 1000–1011.
Hultquist, J.F., Binka, M., LaRue, R.S., Simon, V., Harris, R.S., 2011a. Vif proteins of human and simian immunodeficiency viruses require cellular CBFbeta to degrade APOBEC3 restriction factors. J, Virol, 86 (5), 2874–2877.
Hultquist, J.F., Lengyel, J.A., Refsland, E.W., LaRue, R.S., Lackey, L., Brown, W.L., Harris, R.S., 2011b. Human and rhesus APOBEC3D, APOBEC3F, APOBEC3G, and APOBEC3H demonstrate a conserved capacity to restrict Vif-deficient HIV-1. J. Virol. 85 (21), 11220–11234.
Hultquist, J.F., McDougle, R.M., Anderson, B.D., Harris, R.S., 2012. HIV type 1 viral infectivity factor and the RUNX transcription factors interact with core binding factor beta on genetically distinct surfaces. AIDS Res. Hum. Retroviruses 28 (12), 1543–1551.
Izumi, T., Takaori-Kondo, A., Shirakawa, K., Higashitsuji, H., Itoh, K., Io, K., Matsui, M., Iwai, K., Kondoh, H., Sato, T., Tomonaga, M., Ikeda, S., Akari, H., Koyanagi, Y., Fujita, J., Uchiyama, T., 2009. MDM2 is a novel E3 ligase for HIV-1 Vif. Retrovirology 6, 1.
Jäger, S., Kim, D.Y., Hultquist, J.F., Shindo, K., LaRue, R.S., Kwon, E., Li, M., Anderson, B.D., Yen, L., Stanley, D., Mahon, C., Kane, J., Franks-Skiba, K., Cimermancic, P., Burlingame, A., Sali, A., Craik, C.S., Harris, R.S., Gross, J.D., Krogan, N.J., 2011. Vif hijacks CBF-beta to degrade APOBEC3G and promote HIV-1 infection. Nature 481 (7381), 371–375.
Kim, D.Y., Kwon, E., Hartley, P.D., Crosby, D.C., Mann, S., Krogan, N.J., Gross, J.D., 2013. CBFbeta stabilizes HIV Vif to counteract APOBEC3 at the expense of RUNX1 target gene expression. Mol. Cell 49 (4), 632–644.
Luo, K., Xiao, Z., Ehrlich, E., Yu, Y., Liu, B., Zheng, S., Yu, X.F., 2005. Primate lentiviral virion infectivity factors are substrate receptors that assemble with cullin 5-E3 ligase through a HCCH motif to suppress APOBEC3G. Proc. Nat. Acad. Sci. U.S.A. 102 (32), 11444–11449.
Marin, M., Rose, K.M., Kozak, S.L., Kabat, D., 2003. HIV-1 Vif protein binds the editing enzyme APOBEC3G and induces its degradation. Nat. Med. 9 (11), 1398–1403.
Mehle, A., Goncalves, J., Santa-Marta, M., McPike, M., Gabuzda, D., 2004. Phosphorylation of a novel SOCS-box regulates assembly of the HIV-1 Vif-Cul5 complex that promotes APOBEC3G degradation. Genes Dev. 18 (23), 2861–2866.
Mehle, A., Thomas, E.R., Rajendran, K.S., Gabuzda, D., 2006. A zinc-binding region in Vif binds Cul5 and determines cullin selection. J. Biol. Chem. 281 (25), 17259–17265.
Pery, E., Rajendran, K.S., Brazier, A.J., Gabuzda, D., 2009. Regulation of APOBEC3 proteins by a novel YXXL motif in human immunodeficiency virus type 1 Vif and simian immunodeficiency virus SIVagm Vif. J. Virol. 83 (5), 2374–2381.
Russell, R.A., Pathak, V.K., 2007. Identification of two distinct human immunodeficiency virus type 1 Vif determinants critical for interactions with human APOBEC3G and APOBEC3F. J. Virol. 81 (15), 8201–8210.
Sheehy, A.M., Gaddis, N.C., Choi, J.D., Malim, M.H., 2002. Isolation of a human gene that inhibits HIV-1 infection and is suppressed by the viral Vif protein. Nature 418 (6898), 646–650.
Sheehy, A.M., Gaddis, N.C., Malim, M.H., 2003. The antiretroviral enzyme APOBEC3G is degraded by the proteasome in response to HIV-1 Vif. Nat. Med. 9 (11), 1404–1407.
Shindo, K., Takaori-Kondo, A., Kobayashi, M., Abudu, A., Fukunaga, K., Uchiyama, T., 2003. The enzymatic activity of CEM15/Apobec-3G is essential for the regulation of the infectivity of HIV-1 virion but not a sole determinant of its antiviral activity. J. Biol. Chem. 278 (45), 44412–44416.
Shirakawa, K., Takaori-Kondo, A., Kobayashi, M., Tomonaga, M., Izumi, T., Fukunaga, K., Sasada, A., Abudu, A., Miyauchi, Y., Akari, H., Iwai, K., Uchiyama, T., 2006. Ubiquitination of APOBEC3 proteins by the Vif-Cullin5-ElonginB-ElonginC complex. Virology 344 (2), 263–266.
Stopak, K., de Noronha, C., Yonemoto, W., Greene, W.C., 2003. HIV-1 Vif blocks the antiviral activity of APOBEC3G by impairing both its translation and intracellular stability. Mol. Cell 12 (3), 591–601.
Wolfe, L.S., Stanley, B.J., Liu, C., Eliason, W.K., Xiong, Y., 2010. Dissection of the HIV Vif interaction with human E3 ubiquitin ligase. J Virol 84 (14), 7135–7139.
Yu, X., Yu, Y., Liu, B., Luo, K., Kong, W., Mao, P., Yu, X.F., 2003. Induction of APOBEC3G ubiquitination and degradation by an HIV-1 Vif-Cul5-SCF complex. Science 302 (5647), 1056–1060.
Yu, Y., Xiao, Z., Ehrlich, E.S., Yu, X., Yu, X.F., 2004. Selective assembly of HIV-1 Vif-Cul5-ElonginB-ElonginC E3 ubiquitin ligase complex through a novel SOCS box and upstream cysteines. Genes Dev. 18 (23), 2867–2872.
Zhang, H., Yang, B., Pomerantz, R.J., Zhang, C., Arunachalam, S.C., Gao, L., 2003. The cytidine deaminase CEM15 induces hypermutation in newly synthesized HIV-1 DNA. Nature 424 (6944), 94–98.
Zhang, W., Du, J., Evans, S.L., Yu, Y., Yu, X.F., 2011. T-cell differentiation factor CBF-beta regulates HIV-1 Vif-mediated evasion of host restriction. Nature 481 (7381), 376–379.

STEM CELLS®

TISSUE-SPECIFIC STEM CELLS

C/EBPβ Expressed by Bone Marrow Mesenchymal Stromal Cells Regulates Early B-cell Lymphopoiesis

Satoshi Yoshioka[1,2], Yasuo Miura[2,#], Hisayuki Yao[2], Sakiko Satake[2], Yoshihiro Hayashi[2,3], Akihiro Tamura[2], Terutoshi Hishita[4], Tatsuo Ichinohe[5], Hideyo Hirai[2], Akifumi Takaori-Kondo[1] and Taira Maekawa[2]

[1]Department of Hematology/Oncology, Graduate School of Medicine, Kyoto University and [2]Department of Transfusion Medicine & Cell Therapy, Kyoto University Hospital, Kyoto, 606-8507, Japan. [3]Division of Gastroenterology and Hematology, Shiga University of Medical Science, Shiga, 520-2192, Japan. [4]Department of Hematology, National Himeji Medical Center, Hyogo, 670-8520, Japan. [5] Department of Hematology and Oncology, Research Institute for Radiation Biology and Medicine, Hiroshima University, Hiroshima 734-8553, Japan.

Key Words. B lymphocytes • bone marrow • CCAAT/enhancer-binding protein β • mesenchymal stromal cells.

ABSTRACT

The transcription factor CCAAT/enhancer-binding protein β (C/EBPβ) regulates the differentiation of a variety of cell types. Here, the role of C/EBPβ expressed by bone marrow mesenchymal stromal cells (BMMSCs) in B-cell lymphopoiesis was examined. The size of the precursor B-cell population in bone marrow was reduced in C/EBPβ-knockout (KO) mice. When bone marrow cells from C/EBPβ-KO mice were transplanted into lethally irradiated wild-type (WT) mice, which provide a

Author contributions: S.Y.: conception and design, collection of data, data analysis and interpretation, and manuscript writing; Y.M.: conception and design, financial support, collection of data, data analysis and interpretation, and manuscript writing; H.Y.: conception and design, collection of data, data analysis and interpretation, and manuscript writing; S.S.: collection of data, and data analysis and interpretation; Y.H.: data analysis and interpretation; A.T.: data analysis and interpretation; T.H.: conception and design, collection of data, and data analysis and interpretation; T.I.: conception and design, financial support, data analysis and interpretation, and manuscript writing; H.H.: conception and design, financial support, collection of data, data analysis and interpretation, and manuscript writing; A.T.-K.: conception and design, data analysis and interpretation, and manuscript writing; T.M.: conception and design, financial support, data analysis and interpretation, and manuscript writing. All authors listed approve this manuscript.
[#]Correspondence: Yasuo Miura, M.D., Ph.D. , Address: Department of Transfusion Medicine & Cell Therapy, Kyoto University Hospital, 54 Kawaharacho, Shogoin, Sakyo-ku, Kyoto, 606-8507, Japan., Tel: +81-75-751-3630, Fax: +81-75-751-4283, E-mail: ym58f5@kuhp.kyoto-u.ac.jp;
Grants: This work was supported in part by a Grant-in-Aid from the Ministry of Education, Culture, Sports, Science and Technology in Japan (to Y.M., Y.H., T.I., H.H., and T.M), a Grant-in-Aid from the Japan Science and Technology Agency (to Y.M.), and a Grant-in-Aid from the Ministry of Health, Labour and Welfare in Japan (to T.I. and T. M). This work was also supported in part by the Japan Leukemia Research Fund (to Y.M), the Kyoto University Translational Research Center (to Y.M), the Ichiro Kanehara Foundation (to Y.M. and S.Y.), the National Cancer Center Research and Development Fund (to T.M., 23-A-23), the Kobayashi Foundation for Cancer Research (to T.M.), the Cell Science Research Foundation (to Y.M.), and the Senshin Medical Research Foundation (to T.M.).; Received January 21, 2013; accepted for publication September 05, 2013. 1066-5099/2013/$30.00/0 doi: 10.1002/stem.1555

This article has been accepted for publication and undergone full peer review but has not been through the copyediting, typesetting, pagination and proofreading process which may lead to differences between this version and the Version of Record. Please cite this article as doi: 10.1002/stem.1555

normal bone marrow microenvironment, the size of the precursor B-cell population was restored to a level equivalent to that generated by WT bone marrow cells. In co-culture experiments, BMMSCs from C/EBPβ-KO mice did not support the differentiation of WT c-Kit$^+$ Sca-1$^+$ Lineage$^-$ hematopoietic stem cells (KSL cells) into precursor B-cells, whereas BMMSCs from WT mice did. The impaired differentiation of KSL cells correlated with the reduced production of CXCL12/stromal cell-derived factor-1 by the co-cultured C/EBPβ-deficient BMMSCs. The ability of C/EBPβ-deficient BMMSCs to undergo osteogenic and adipogenic differentiation was also defective. The survival of leukemic precursor B-cells was poorer when they were co-cultured with C/EBPβ-deficient BMMSCs than when they were co-cultured with WT BMMSCs. These results indicate that C/EBPβ expressed by BMMSCs plays a crucial role in early B-cell lymphopoiesis.

INTRODUCTION

Early B-cell lymphopoiesis occurs in bone marrow, during which hematopoietic cells in the bone marrow interact with non-hematopoietic cells in the bone marrow microenvironment [1]. The molecular mechanisms in hematopoietic cells that underlie early B-cell lymphopoiesis have been well investigated. Several transcription factors in hematopoietic cells are essential for early B-cell lymphopoiesis such as PU.1, Ikaros, E2A, early B-cell factor, and paired box protein 5 [2]. By contrast, the transcription factors in non-hematopoietic cells that are important for early B-cell lymphopoiesis remain unclear.

The transcription factor CCAAT/enhancer-binding protein (C/EBPβ) is crucial for the differentiation of a variety of cell types, including adipocytes [3], hepatocytes, keratinocytes and mammary epithelial cells [4, 5]. C/EBPβ regulates myelopoiesis and granulopoiesis in hematopoiesis [6-8]. However, the role(s) of C/EBPβ expressed by bone marrow mesenchymal stromal cells (BMMSCs), one of the major hematopoiesis-supporting cellular constituents in the bone marrow microenvironment [9-11], in B-cell lymphopoiesis is unknown. In this study, detailed analysis of B-cell subpopulations in C/EBPβ-knockout (KO) mice revealed that the level of precursor B-cells was decreased in the bone marrow of C/EBPβ-KO mice. The bone marrow microenvironment, rather than hematopoietic cells, contributed to the defective generation of precursor B-cells in C/EBPβ-KO mice. C/EBPβ-deficient BMMSCs did not support the differentiation of precursor B-cells from hematopoietic stem cells (HSCs), whereas BMMSCs from wild-type (WT) mice did. In addition, the proliferation and survival of leukemic precursor B-cells co-cultured with C/EBPβ-deficient BMMSCs was examined.

MATERIALS AND METHODS

Mice. C57BL/6 (Ly5.2) and SCID (C.B-17/Icr-*scid/scid*Jcl) mice were purchased from CLEA Japan. C/EBPβ-KO (Ly5.2) mice [12] were back-crossed to C57BL/6 (Ly5.2) mice at least eight times. C/EBPβ-KO (Ly5.2)

mice and WT (Ly5.2) mice were obtained by intercrossing heterozygous (C/EBPβ$^{+/-}$) mice. Transgenic GFP-expressing (GFP^{+}) mice were kindly provided by Dr. Masaru Okabe (Osaka University) [13]. To obtain GFP^{+} C/EBPβ-KO and GFP^{+} WT mice, GFP+ mice were crossed with C/EBPβ$^{+/-}$ mice. C57BL/6 (Ly5.1) mice were kindly provided by Dr. Shigekazu Nagata (Kyoto University). All mice used in the experiments were 7–12 weeks old. All mice were maintained under specific pathogen-free conditions at the Institute of Laboratory Animals, Kyoto University. All animal experiments were approved by the Committee on Animal Research of the Kyoto University Faculty of Medicine.

Bone marrow transplantation. Bone marrow cells (1×10^6 cells/mouse) were administrated intravenously through the tail vein into WT mice that received 10 Gy of total body irradiation prior to transplantation. For competitive transplantation experiments, lethally irradiated (10 Gy) WT mice received bone marrow cells from both GFP^{-} WT mice (1×10^6 cells/mouse) and either GFP^{+} C/EBPβ-KO or GFP^{+} WT mice (1×10^6 cells/mouse). B-cell lymphopoiesis was evaluated by flow cytometric analysis at 14–20 weeks after transplantation.

BMMSC culture and in vivo bone formation assays. Murine BMMSCs were isolated as previously described [14-16]. Briefly, murine bone marrow cells (1.5×10^7) from long bones was seeded into 10 cm culture dishes, incubated for 3 hours at 37°C to allow adherent cells to attach, and then washed twice with PBS to remove non-adherent cells. BMMSCs formed adherent colonies and adherent cells were collected after 12–15 days of culture. Primary cultures were passaged to disperse the colony-forming cells (passage 1). Cells at passage 1 were used in experiments. The culture medium consisted of α-MEM supplemented with 20% fetal bovine serum (FBS), 2 mM L-glutamine, 100 U/mL penicillin, 100 μg/mL streptomycin, and 55 μM 2-mercaptoethanol (all from Gibco-BRL). For osteogenic induction *in vitro*, 2 mM β-glycerophosphate (Sigma), 100 μM L-ascorbic acid 2-phosphate (Wako Pure Chemical Industries Ltd.), and 10 nM dexamethasone (Sigma) were added to the culture media. Calcium deposition was evaluated by staining with 1% Alizarin Red S after 4 weeks of osteogenesis-inducing culture. For adipogenic induction *in vitro*, 0.5 mM isobutylmethylxanthine, 60 μM indomethacin, 0.5 μM hydrocortisone and 10 μg/mL insulin were added to the culture media. Oil Red O staining was used to assess lipid-laden fat cells after 1–2 week of adipogenesis-inducing culture. The area of the mineralized areas and the number of Oil Red O^{+} cells were quantitated using Image J software. In some experiments, the differentiated BMMSCs were used in further experiments, including immunoblot analysis or quantitative real-time PCR to analyze the expression of osteogenesis- or adipogenesis-associated molecules. For *in vivo* bone formation assays, cultured BMMSCs ($1–4\times10^6$ cells) were mixed with 40 mg of hydroxyapatite/tricalcium phosphate (HA/TCP) ceramic powder (Zimmer). The mixture was implanted subcutaneously into the dorsal surface of 7–9-weeks-old SCID mice, and the implants were harvested 8 weeks later. Histological analysis and quantification of bone

formation in the harvested implants were performed as previously described [17, 18]. Human bone marrow samples were obtained with informed consent and the approval of the ethical committee of Kyoto University Hospital. Human BMMSCs were isolated from bone marrow samples as previously described [19, 20] and cultured in α-MEM containing 15% FBS, 100 μM L-ascorbic acid 2-phosphate, 2 mM L-glutamine, 100 U/mL penicillin, and 100 μg/mL streptomycin. To exclude the possibility that hematopoietic cells in BMMSC cultures affect the results, $CD45^+$ cells were isolated from primary cultures of BMMSCs using anti-CD45 immunomagnetic microbeads (Miltenyi Biotech). These cells did not have multi-differentiation capabilities *in vitro* and did not express C-X-C motif chemokine 12 (CXCL12) / stromal cell-derived factor-1 (SDF-1), stem cell factor (SCF), and interleukin-7 (IL-7), whereas CD45- cells did (Fig. S1). In some experiments, human bone marrow cells and BMMSCs were purchased from AllCells or Lonza. The clinical features of the precursor B-cell acute lymphoblastic leukemia (B-ALL) samples are shown in Table S2.

Sorting of KSL cells and co-culture of KSL cells with BMMSCs. Single-cell suspensions of bone marrow cells from WT (Ly5.1) mice were labeled with allophycocyanin (APC)-conjugated anti-mouse c-Kit (2B8), fluorescein isothiocyanate (FITC)-conjugated anti-mouse Ly6A/E [Sca-1] (D7), and PerCP-Cy5.5-conjugated anti-mouse lineage markers, including CD3e (145-2C11), CD4 (RM4-5), CD8 (53-6.7), CD19 (1D3), B220 (RA3-6B2), CD11b (M1/70), Gr-1 (RB6-8C5) and Ter119 (TER119). All antibodies were purchased from eBioscience. Sorting of c-Kit^+ Sca-1^+ Lineage- (KSL) HSCs was performed with a FACSAria cell sorter (Becton Dickinson). KSL cells (1×10^4) were co-cultured with BMMSCs (2×10^6) in 3 mL of RPMI 1640 supplemented with 10% FBS, 2 mM L-glutamine, 100 U/mL penicillin, 100 μg/mL streptomycin, 10 ng/mL SCF, 10 ng/mL fms-like tyrosine kinase 3-ligand (Flt3-L), and 10 ng/mL IL-7 in a 6 cm dish. The medium was replenished after 6 days, and B-cell lymphopoiesis was analyzed after 10 days of co-culture. For CXCL12/SDF-1 rescue experiments, recombinant CXCL12/SDF-1 (R&D Systems) was added to the medium to be a final concentration of 10 ng/mL.

Co-culture of murine precursor B-ALL cells with BMMSCs. Murine precursor B-ALL cells, BaF3 that were transfected with Bcr/Abl^{p185} (BaF3/Bcr-Abl), were generated as previously described [21]. BaF3/Bcr-Abl cells were co-cultured with BMMSCs derived from either C/EBPβ-KO or WT mice using a co-culture system as previously reported [22]. BMMSCs (1×10^6) were attached to the reverse side of the membrane of a 6-well cell culture insert (BD Falcon) and cultured for 3 days. Then, BaF3/Bcr-Abl cells (5×10^4) were seeded onto the upper side of the insert membrane. In co-culture experiments, cells were cultured in RPMI medium containing 10% FBS, 2 mM L-glutamine, 100 U/mL penicillin, and 100 μg/mL streptomycin. The number of BaF3/Bcr-Abl cells on the upper side of the insert was counted after 3 days of co-culture. BaF3/Bcr-Abl cells were stained with propidium iodide (PI) after 2 days of co-culture

to label DNA for cell cycle analysis. After co-culture with BMMSCs for 3 days, the percentage of apoptotic BaF3/Bcr-Abl cells was determined by performing APC-conjugated Annexin V and PI (BD Bioscience) co-staining according to the manufacturer's instructions.

BrdU incorporation assay. BaF3/Bcr-Abl cells (2×10^4 cells/well in a 96-well plate) were cultured in the medium supplemented with 0, 0.01, 0.1, 1, or 10 ng/mL CXCL12/SDF-1. After 24 hours of culture, BrdU incorporation was analyzed by using the colorimetric immunoassay Cell Proliferation ELISA, BrdU (Roche Applied Science) according to the manufacturer's instructions.

Flow cytometric analysis. Single-cell suspensions of bone marrow cells were stained with fluorescence-conjugated antibodies and analyzed with a FACSCanto II (Becton Dickinson). B-cell populations were identified based on the Hardy Fraction [23]. The antibodies used were FITC-conjugated anti-mouse CD43 (R2/60), FITC-conjugated anti-mouse CD45.1/Ly5.1 (A20), phycoerythrin (PE)-conjugated anti-mouse BP-1 (6C3), PE-conjugated anti-mouse IgD (11-26c), APC-conjugated anti-mouse B220 (RA3-6B2), APC-conjugated anti-mouse CD11b (M1/70), PE-Cy7-conjugated anti-mouse CD24 (M1/69), and PE-Cy7-conjugated anti-mouse IgM (II/41). All antibodies were purchased from eBioscience. Dead cells were excluded by staining with PI. Data were analyzed using FlowJo software (Tree Star).

Quantitative real-time PCR. Total RNA was extracted using the QIAamp RNA Blood Mini Kit (Qiagen). cDNA was prepared using the PrimeScript RT reagent kit (Perfect Real-Time) (Takara). Real-time PCR was performed using the StepOnePlus real-time PCR system (Applied Biosystems) and a Universal ProbeLibrary (Roche). The primer sets and universal probes used are listed in Table S1. Gene expression levels were normalized to the mRNA level of glyceraldehyde-3-phosphate dehydrogenase (GAPDH). All samples were analyzed in duplicate.

Immunoblot analysis. Cells lysates were boiled in SDS sample buffer, separated by SDS-PAGE, and transferred to PVDF membranes. Primary antibodies against runt-related transcription factor 2 (Runx2, Abcam), alkaline phosphatase (ALP, Abcam), lipoprotein lipase (Lpl, Abcam), fatty acid-binding protein 4 (FABP4, Abcam), peroxisome proliferator-activated receptor γ (PPARγ, Cell Signaling Technology), and β-actin (Sigma-Aldrich) were used. Immunoreactive proteins were detected using horseradish peroxidase-conjugated anti-mouse (for anti-Runx2, -Lpl, and -β-actin) or anti-rabbit (for anti-ALP, -PPARγ, and -FABP4) immunoglobulin G (GE Healthcare) and visualized using enhanced chemiluminescence or enhanced chemiluminescence prime kits (GE Healthcare). Relative protein expression levels were measured using Quantity One software (Bio-Rad).

Histological analysis. Histological analysis and quantification of bone formation were

performed as previously described [17]. Briefly, bone specimens from the lower vertebrae of mice were stained with hematoxylin and eosin (HE), and trabecular bone areas were measured at 100× magnification using Image J software. Images were acquired using a DP71 digital camera and DP Controller software in combination with a CX41 microscope and a PlanCN objective lens (10×, 0.25 numerical aperture) (Olympus).

CXCL12/SDF-1 ELISA. Culture supernatant was collected after culturing murine BMMSCs (2×10^6 cells in 3mL per dish) for 3 days, or after co-culturing WT KSL cells with the same number of BMMSCs for 10 days in 6 cm dishes. The level of CXCL12/SDF-1 protein in the culture supernatant was measured using the Quantikine mouse CXCL12/SDF-1α ELISA kit (R&D Systems) according to the manufacturer's instructions.

Statistical analyses. The unpaired Student's *t*-test was used for analysis. Data in bar graphs indicate the mean ± SD, and statistical significance is expressed as follows: *, $P < 0.05$; **, $P < 0.01$; n.s., not significant.

RESULTS

The level of precursor B-cells is decreased in the bone marrow of C/EBPβ-KO mice.

The levels of B-cell subsets in C/EBPβ-KO mice were analyzed by flow cytometric analysis based on the expression patterns of B220, CD43, BP-1, CD24, surface IgM (sIgM), and surface IgD (sIgD) [23]. The percentage of $B220^+$ B-cells in the bone marrow was significantly lower in C/EBPβ-KO mice than in WT mice (Fig. 1A: WT, 26.5 ± 7.3%; C/EBPβ-KO, 19.1 ± 7.1%; *P < 0.05). The percentage of $B220^+$ B-cells in the spleen was similar in WT and C/EBPβ-KO mice (Fig. S2A–C), which is consistent with a previous study [24]. The percentage of B220+CD43+ precursor B-cells in the bone marrow was significantly lower in C/EBPβ-KO mice than in WT mice (Fig. 1B). In detail, the percentages of pre-pro-B-cells ($B220^+CD43^+BP\text{-}1^-CD24^-$; Fraction A), pro-B-cells ($B220^+CD43^+BP^-1^-CD24^+$ and $B220^+CD43^+BP^-1^+CD24^{low}$; Fraction B/C), and pre-BI cells ($B220^+CD43^+BP\text{-}1^+CD24^{high}$; Fraction C') were all significantly lower in C/EBPβ-KO mice than in WT mice (Fig. 1C, D). The percentages of pre-BII cells ($B220^+CD43^-sIgM^-sIgD^-$; Fraction D), immature B-cells ($B220^+CD43^-sIgM^+sIgD^{low}$; Fraction E), and mature B-cells ($B220^+CD43^+sIgM^+sIgD^{high}$; Fraction F) in bone marrow were not significantly different between C/EBPβ-KO mice and WT mice (Fig. S3A, B).

The bone marrow microenvironment contributes to the impairment of B-cell lymphopoiesis in C/EBPβ-KO mice.

The bone marrow microenvironment is crucial for early B-cell development [1]; therefore, we hypothesized that the bone marrow microenvironment contributes to the decreased level of precursor B-cells in C/EBPβ-KO mice. We conducted bone marrow transplantation experiments to test this hypothesis (Fig. 2A). Bone marrow cells from C/EBPβ-KO mice were transplanted into lethally irradiated (10 Gy) WT mice (KO→WT). As a control, bone marrow cells from WT mice were transplanted

into WT mice (WT→WT). The recipient WT mice should provide a normal bone marrow microenvironment. Fourteen weeks after transplantation, the percentage of B220+ B-cells in bone marrow was similar in recipients that received C/EBPβ-deficient bone marrow cells and those who received WT bone marrow cells (Fig. 2B). Detailed analysis of B-cell subsets showed that the levels of pre-pro B-cells (Fraction A), pro-B-cells (Fraction B/C), and pre-BI cells (Fraction C') were similar in the two groups (Fig. 2C). The size of the B-cell population in the spleen was similar in both groups (Fig. S4*A*, B).

Next, we performed competitive bone marrow transplantation experiments. The same number of GFP^- WT bone marrow cells and either GFP^+ WT bone marrow cells (Transplantation-A) or GFP^+ C/EBPβ-deficient bone marrow cells (Transplantation-B) were co-transplanted into lethally irradiated WT mice (Fig. 2D). GFP^+ C/EBPβ-deficient hematopoietic cells engrafted into recipient bone marrow with approximately 50% cellularity (Fig. 2E, BM, Transplantation-B), which was equivalent to the engraftment rate of GFP^+ WT hematopoietic cells (Fig. 2E, BM, Transplantation-A). The percentage of GFP^+ cells in the spleens of recipients was also similar in both transplantations (Fig. 2E, SP). GFP^+ C/EBPβ-deficient bone marrow cells and GFP^- WT bone marrow cells gave rise to a similar percentage of $B220^+$ B-cells in the recipient bone marrow when they were co-transplanted (Fig. 2F, Transplantation-B, open bar versus closed bar). GFP^+ WT bone marrow cells and GFP^- WT bone marrow cells also generated a similar percentage of $B220^+$ B-cells (Fig. 2F, Transplantation-A, dotted bar versus closed bar). These findings demonstrate that C/EBPβ-deficient bone marrow hematopoietic cells are able to generate B-cells as efficiently as normal WT bone marrow hematopoietic cells when transplanted into a normal bone marrow microenvironment. Taken together, these results indicate that the impairment of B-cell lymphopoiesis in C/EBPβ-KO mice is due, at least in part, to the bone marrow microenvironment.

Reverse transplantation from WT mice to C/EBPβ-KO mice was also performed (Fig. S5A). However, donor-derived (Ly5.1) B-cell reconstitution after transplantation could not be evaluated in most C/EBPβ-KO recipient mice because of early death, although an irradiation dose was reduced. When an irradiation dose of 5 Gy was used, donor cells did not engraft (Fig. S5B, C). When an irradiation dose of 7 Gy was used, the level of donor-derived (Ly5.1) $B220^+$ cells in peripheral blood and the bone marrow was lower in surviving C/EBPβ-KO recipients than in WT recipients (Fig. S5D, E). Perhaps the C/EBPβ-deficient bone marrow microenvironment cannot support hematopoietic and/or immune recover after transplantation.

C/EBPβ-deficient BMMSCs have an impaired ability to support the differentiation of HSCs into precursor B-cells.

BMMSCs are important for the regulation of B-cell lymphopoiesis in the bone marrow microenvironment [1, 11, 25]; therefore, we explored whether C/EBPβ-deficient BMMSCs have an impaired ability to support B-cell

lymphopoiesis. KSL HSCs from the bone marrow of WT (Ly5.1) mice (WT-KSL cells) were co-cultured with BMMSCs from C/EBPβ-KO (Ly5.2) mice in the presence of SCF, Flt3-L, and IL-7 (Fig. 3A). BMMSCs from WT (Ly5.2) mice were used as a control in the co-culture experiments (Fig. 3A). The generation of hematopoietic cells from WT-KSL cells was significantly lower when cells were co-cultured with C/EBPβ-deficient BMMSCs than when they were co-cultured with WT BMMSCs (Fig. 3B). The generation of $B220^+$ B-cells from WT-KSL cells was also significantly lower when cells were co-cultured with C/EBPβ-deficient BMMSCs than when they were co-cultured with WT BMMSCs (Fig. 3C, D and S6A). Detailed analysis of B-cell subsets showed that differentiation of WT-KSL cells into precursor B-cells was reduced (Fig. 3E, left panels) and differentiation from pre-pro-B-cells (Fraction A) to pro-B-cells/pre-BI cells (Fraction B/C/C') was suppressed when cells were co-cultured with C/EBPβ-deficient BMMSCs compared to when they were co-cultured with WT BMMSCs (Fig. 3E, right panels and 3F). Therefore, C/EBPβ-deficient BMMSCs have an impaired ability to support the differentiation of normal HSCs into precursor B-cells.

Reduced production of CXCL12/SDF-1 by C/EBPβ-deficient BMMSCs partially contributes to impaired differentiation of HSCs into B-cells.

Next, the expression of B-cell lymphopoiesis-associated humoral factors in BMMSCs was examined. Levels of CXCL12/SDF-1 (Fig. 3G) and Flt3-L (Fig. S6C) mRNA were significantly lower in C/EBPβ-deficient BMMSCs than in WT BMMSCs. Levels of IL-7 (Fig. S6D) and SCF (Fig. S6E) mRNA tended to be lower in C/EBPβ-deficient BMMSCs than in WT BMMSCs, although the difference was not statistically significant. CXCL12/SDF-1 is essential for hematopoiesis, particularly B-cell lymphopoiesis [26, 27]. In addition to mRNA expression, the protein concentration of CXCL12/SDF-1 was significantly lower in the culture supernatant of C/EBPβ-deficient BMMSCs than that of WT BMMSCs (WT, $n = 5$, 9.90 ± 1.93 ng/mL; C/EBPβ-deficient, $n = 5$, 4.47 ± 1.16 ng/mL; $^{**}P < 0.01$) (Fig. 3H). The concentration of CXCL12/SDF-1 in the supernatant of BMMSC co-cultures correlated with the number of $B220^+$ B-cells that differentiated from WT-KSL cells (Fig. 3I). The addition of exogenous CXCL12/SDF-1 to the co-culture of C/EBPβ-deficient BMMSCs and WT-KSL cells slightly increased the total number of cells and the number of B-cells (Fig. 3B, D). The frequencies of pre-pro-B cells, pro-B and pre-BI cells (Fractions A, B and C+C') that differentiated from KSL cells were not apparently affected by the addition of CXCL12/SDF-1 to the culture medium (Fig. S6A, B). Thus, reduced production of CXCL12/SDF-1 by C/EBPβ-deficient BMMSCs is partially associated, and other functional abnormalities of C/EBPβ-deficient BMMSCs may be associated with the impaired differentiation of HSCs into B-cells in the co-culture.

C/EBPβ-deficient BMMSCs have an impaired multi-differentiation capability.

We sought to identify other differentiation characteristics in which C/EBPβ-deficient

BMMSCs were defective. The ability to differentiate into multiple cell types is a fundamental property of bone marrow mesenchymal stem cells [28, 29]; therefore, C/EBPβ-deficient BMMSCs were evaluated in osteogenic and adipogenic differentiation assays. When BMMSCs were cultured under osteogenesis-inducing conditions *in vitro*, calcium accumulation was significantly lower in C/EBPβ-deficient BMMSCs than in WT BMMSCs, as assessed by Alizarin Red S staining (Fig. 4A, B). The expression of the osteogenic master molecule Runx2 and of another crucial osteogenic marker ALP was down-regulated in C/EBPβ-deficient BMMSCs in this assay (Fig. 4C, D). Moreover, when BMMSCs were subcutaneously implanted with HA/TCP into SCID mice, C/EBPβ-deficient BMMSCs induced less bone formation than WT BMMSCs (Fig. 4E, F). Therefore, the osteogenic differentiation capability of C/EBPβ-deficient BMMSCs was defective compared to that of WT BMMSCs. Findings of skeletal examinations of C/EBPβ-KO mice were in agreement with this. Male and female C/EBPβ-KO mice had a shorter crown-rump length and total length than sex- and age-matched WT mice (Fig. S7A, B). C/EBPβ-KO mice had less trabecular bone (TB) and fewer bone-lining cells on the surface of TB that were positive for osteocalcin, a marker of osteoblasts, than age-matched WT mice (Fig. S7C-F). Next, *in vitro* adipogenic differentiation assays were performed. When BMMSCs were cultured under adipogenesis-inducing conditions *in vitro*, lipid deposition was significantly lower in C/EBPβ-deficient BMMSCs than in WT BMMSCs (Fig. 5A-C). Furthermore, expression of the adipogenic markers PPARγ, Lpl, and Fabp4 was down-regulated in C/EBPβ-deficient BMMSCs in this assay (Fig. 5D, E). Therefore, the adipogenic differentiation capability of C/EBPβ-deficient BMMSCs was defective compared to that of WT BMMSCs.

Taken together, these results demonstrate that C/EBPβ-deficient BMMSCs have an impaired multi-differentiation capability.

Survival of leukemic precursor B-cells is suppressed when co-cultured with C/EBPβ-deficient BMMSCs.

The results described so far demonstrate that C/EBPβ expressed by BMMSCs plays a crucial role in supporting physiological early B-cell lymphopoiesis; therefore, we explored whether C/EBPβ expressed by BMMSCs is involved in the proliferation and survival of leukemic precursor B-cells. The murine precursor B-ALL cell line BaF3/Bcr-Abl was co-cultured with BMMSCs from C/EBPβ-KO or WT mice (Fig. 6A). The number of BaF3/Bcr-Abl cells was higher when they were co-cultured with WT BMMSCs than when they were cultured alone (Fig. 6B). However, the number of BaF3/Bcr-Abl cells was similar when they were co-cultured with C/EBPβ-deficient BMMSCs and when they were cultured alone (Fig. 6B). This difference was not associated with cell cycle (Fig. 6C, D). The proportion of apoptotic BaF3/Bcr-Abl cells was significantly higher when they were co-cultured with C/EBPβ-deficient BMMSCs than when they were co-cultured with WT BMMSCs (Fig. 6E, F). Production of CXCL12/SDF-1 was reduced in C/EBPβ-deficient BMMSCs (Fig. 3G, H);

therefore, the response of BaF3/Bcr-Abl cells to CXCL12/SDF-1 was examined. Stimulation with CXCL12/SDF-1 increased the BrdU incorporation of BaF3/Bcr-Abl cells in a dose-dependent manner (Fig. 6G). These results suggest that reduced production of CXCL12/SDF-1 and impaired anti-apoptotic activity in C/EBPβ-deficient BMMSCs contribute to the reduced survival of BaF3/Bcr-Abl cells. In human BMMSCs derived from precursor B-ALL bone marrow samples, the mRNA levels of C/EBPβ and CXCL12/SDF-1 were increased in some cases (Fig. S8A, B). Thus, the expression level of C/EBPβ in BMMSCs might modulate the survival of leukemic precursor B-cells.

DISCUSSION

In this study, we showed that the bone marrow microenvironment contributed to the reduced level of precursor B-cells in the bone marrow of C/EBPβ-KO mice, and that C/EBPβ-deficient BMMSCs had an impaired ability to support differentiation of HSCs into precursor B-cells and an impaired multi-differentiation capability. We and others have previously shown that myelopoiesis and the number of hematopoietic stem and progenitor cells are comparable between C/EBPβ-KO and WT mice [6, 8]. Therefore, impaired B-cell lymphopoiesis in C/EBPβ-KO mice is not due to a reduced level of HSCs and is not associated with increased myelopoiesis.

It was previously reported that reduced production of IL-7 by bone marrow stromal cells and weak response of $B220^{+}IgM^{-}$ B-cells to IL-7 contribute to the impairment of B-cell lymphopoiesis in C/EBPβ-KO mice [24]. In this study, the expression of IL-7 tended to be lower in C/EBPβ-deficient BMMSCs than in WT BMMSCs; however, this difference was not statistically significant. Rather, C/EBPβ-deficient bone marrow hematopoietic cells were able to generate B-cells as efficiently as normal WT bone marrow hematopoietic cells when they were transplanted into the normal bone marrow microenvironment of WT mice. This finding demonstrates that the bone marrow microenvironment, rather than hematopoietic cells, is responsible for the impairment of B-cell lymphopoiesis in C/EBPβ-KO mice, at least at steady-state. The contributions of hematopoietic cells and the bone marrow microenvironment to the impairment of B-cell lymphopoiesis in C/EBPβ-KO mice reported here differ from those previously reported [24]; however, the reason(s) for this discrepancy is unclear. The two reports used different methods to evaluate B-cell generation; *in vitro* liquid culture was performed in the previous report [24] and *in vivo* reconstitution following hematopoietic cell transplantation was performed in our analysis. IL-7 is an essential cytokine for early B-cell lymphopoiesis that is expressed in the bone marrow microenvironment [30], and C/EBPβ-deficient hematopoietic cells exhibit impaired responses to various cytokines in addition to IL-7 [7]. Thus, both the bone marrow microenvironment and hematopoietic cells might contribute to the impairment of B-cell lymphopoiesis in C/EBPβ-KO mice, and the relative contribution of each might vary in different states.

Transcription factors expressed by hematopoietic cells that are essential for early B-cell lymphopoiesis have been well studied [2]. Whereas WT BMMSCs supported the differentiation of normal purified HSCs (WT-KSL cells) into precursor B-cells in co-culture experiments, C/EBPβ-deficient BMMSCs did not. Therefore, the ability of BMMSCs to support early B-cell lymphopoiesis is dependent upon C/EBPβ. Production of CXCL12/SDF-1 was reduced in C/EBPβ-deficient BMMSCs, and the level of differentiation of normal HSCs into precursor B-cells correlated with the concentration of CXCL12/SDF-1 in the supernatant of BMMSC and HSC co-cultures. Several lines of evidence indicate that CXCL12/SDF-1 has essential roles in early B-cell lymphopoiesis [26, 27, 31]. The current study did not investigate transcriptional regulation of CXCL12/SDF-1 by C/EBPβ directly; however, previous reports demonstrated that C/EBPβ is one of the major regulatory elements driving transcription of CXCL12/SDF-1 [32, 33]. The addition of exogenous CXCL12/SDF-1 to the co-culture of C/EBPβ-deficient BMMSCs and WT-KSL cells slightly increased the total number of B-cells. Hematopoiesis is regulated by the complicated interaction between hematopoietic cells and the bone marrow microenvironment via adhesion molecules and humoral factors including Flt3-L, IL-7, SCF [1, 10, 11]. Reduced production of CXCL12/SDF-1 by C/EBPβ-deficient BMMSCs is partially associated, but other functional abnormalities of C/EBPβ-deficient BMMSCs may be associated with the impaired differentiation of HSCs into B-cells in the co-culture. Further studies are needed to elucidate the contribution of C/EBPβ in BMMSCs to B-cell lymphopoiesis.

BMMSCs are multi-potent non-hematopoietic cells capable of differentiating into a variety of cell types, including osteoblasts, adipocytes and chondrocytes [34-37]. Given that C/EBPβ-deficient BMMSCs had an impaired ability to support B-cell lymphopoiesis, we hypothesized that their multi-differentiation capability was also impaired. C/EBPβ-deficient BMMSCs had an impaired osteogenic differentiation capability compared to WT BMMSCs, which was observed concomitant with reduced expression of the osteogenic master molecule Runx2 *in vitro*, and reduced formation of TB bone and a reduced number of osteoblasts *in vivo*. Moreover, C/EBPβ-deficient BMMSCs had an impaired adipogenic differentiation capability compared to WT BMMSCs. In summary, C/EBPβ-deficient BMMSCs have an impaired ability to support B-cell lymphopoiesis and reduced osteogenic/adipogenic differentiation capabilities; thus, C/EBPβ is presumably an important regulatory transcription factor needed for BMMSCs to exert their biological effects. Several links have been reported between B-cell lymphopoiesis and osteogenic/adipogenic cells. Osteoblasts support B-cell differentiation and commitment from HSCs [38]. Furthermore, CXCL12 abundant reticular cells, which have characteristics of adipo-osteogenic progenitors, are essential for the proliferation and survival of precursor B-cells [25, 39]. The impaired osteogenic and adipogenic differentiation capabilities of C/EBPβ-deficient BMMSCs seem to be associated with their impaired ability to support B-cell lymphopoiesis.

Recently, the contribution of the bone marrow microenvironment to leukemogenesis and chemo-resistance, called the "leukemic niche", has been clarified [40-43]. The association of the leukemic niche with pathogenesis and its potential as a therapeutic target in precursor B-ALL have also been described [44-46]. In the present study, the survival of precursor B-ALL cells was suppressed when they were co-cultured with C/EBPβ-deficient BMMSCs which produced CXCL12/SDF-1 less than WT BMMSCs. The involvement of CXCL12/SDF-1 in the suppressive effect of C/EBPβ-deficient BMMSCs on BaF3/Bcr-Abl cell survival is in agreement with several studies reporting that the CXCL12 (SDF-1)/CXCR4 axis contributes to the pathogenesis of precursor B-ALL [47-49]. In addition, our cell cycle analyses are consistent with a previous study reporting that the promotion of cell survival through CXCL12 (SDF-1)/CXCR4 axis is independent of cell cycle progression [49]. Several CXCL12/CXCR4 antagonists have been investigated as leukemic niche-targeting therapies [47, 49]. C/EBPβ is a regulator of CXCL12/SDF-1 [32, 33]; therefore, C/EBPβ might also be a therapeutic target in some cases in which C/EBPβ is highly expressed in BMMSCs. The anti-apoptotic activity of mesenchymal stem cells in some conditions has been reported [50], although the detail mechanism underlying this remains unknown. Further studies are needed to elucidate the anti-apoptotic effect of BMMSCs on precursor B-ALL cells. Among the various adult hematological malignancies, precursor B-ALL remains difficult to treat with conventional chemotherapy. Better understanding of the contribution of altered C/EBPβ expression in BMMSCs to the pathogenesis of precursor B-ALL may help identify a novel therapeutic target(s) for this disease.

CONCLUSION

C/EBPβ expressed by BMMSCs regulates B-cell lymphopoiesis, particularly precursor B-cell differentiation. In co-culture experiments, survival of leukemic precursor B-cells is associated with the expression level of C/EBPβ in BMMSCs. Further studies are needed to elucidate the contribution of C/EBPβ in BMMSCs to the regulation of physiological and pathological B-cell lymphopoiesis in the bone marrow microenvironment.

ACKNOWLEDGMENTS

We thank Ms. Yoko Nakagawa and Ms. Yoshiko Manabe for their excellent technical assistance.

Disclosure of potential conflicts of interest

The authors have no potential conflicts of interest.